

## Temperature and carrier-density dependence of Auger and radiative recombination in nitride optoelectronic devices

This content has been downloaded from IOPscience. Please scroll down to see the full text.

2013 New J. Phys. 15 125006

(<http://iopscience.iop.org/1367-2630/15/12/125006>)

View [the table of contents for this issue](#), or go to the [journal homepage](#) for more

Download details:

IP Address: 169.231.95.32

This content was downloaded on 19/09/2014 at 14:50

Please note that [terms and conditions apply](#).

## Temperature and carrier-density dependence of Auger and radiative recombination in nitride optoelectronic devices

Emmanouil Kioupakis<sup>1,3</sup>, Qimin Yan<sup>2</sup>, Daniel Steiauf<sup>2</sup>  
and Chris G Van de Walle<sup>2</sup>

<sup>1</sup> Department of Materials Science and Engineering, University of Michigan, Ann Arbor, MI 48109-2136, USA

<sup>2</sup> Materials Department, University of California, Santa Barbara, CA 93106-5050, USA

E-mail: [kioup@umich.edu](mailto:kioup@umich.edu)

*New Journal of Physics* **15** (2013) 125006 (14pp)

Received 28 July 2013

Published 5 December 2013

Online at <http://www.njp.org/>

doi:10.1088/1367-2630/15/12/125006

**Abstract.** Nitride light-emitting diodes are a promising solution for efficient solid-state lighting, but their performance at high power is affected by the efficiency-droop problem. Previous experimental and theoretical work has identified Auger recombination, a three-particle nonradiative carrier recombination mechanism, as the likely cause of the droop. In this work, we use first-principles calculations to elucidate the dependence of the radiative and Auger recombination rates on temperature, carrier density and quantum-well confinement. Our calculated data for the temperature dependence of the recombination coefficients are in good agreement with experiment and provide further validation on the role of Auger recombination in the efficiency reduction. Polarization fields and phase-space filling negatively impact device efficiency because they increase the operating carrier density at a given current density and increase the fraction of carriers lost to Auger recombination.

<sup>3</sup> Author to whom any correspondence should be addressed.



Content from this work may be used under the terms of the [Creative Commons Attribution 3.0 licence](https://creativecommons.org/licenses/by/3.0/). Any further distribution of this work must maintain attribution to the author(s) and the title of the work, journal citation and DOI.

## Contents

<b>1. Introduction</b>	<b>2</b>
<b>2. Auger recombination in nitride semiconductors</b>	<b>4</b>
<b>3. Auger recombination in quantum wells</b>	<b>6</b>
<b>4. Radiative recombination</b>	<b>8</b>
<b>5. Discussion</b>	<b>9</b>
<b>6. Conclusion</b>	<b>11</b>
<b>Acknowledgments</b>	<b>12</b>
<b>References</b>	<b>12</b>

## 1. Introduction

Light-emitting diodes (LEDs) based on the group-III-nitride materials are energy-efficient, nontoxic and long-lasting light sources that can replace incandescent and fluorescent light bulbs for general lighting [1]. Technological advances since the fabrication of the first viable nitride LED in 1993 [2] have enabled solid-state lighting to be a viable solution for display and illumination applications [3]. Despite their commercial success, nitride LEDs are still affected by efficiency issues. The remarkable energy efficiency of nitride LEDs is only achieved at low injected current densities, and it decreases dramatically when operating at the high power needed for lighting. This effect, known as the *efficiency-droop* problem [4], is a universal feature of nitride LEDs that becomes progressively worse for longer-wavelength devices (*green gap*). Mitigating the efficiency-droop and green-gap problems will reduce the cost of high-power nitride LEDs and accelerate the wider adoption of solid-state lighting.

The origin of the efficiency-droop problem remains a subject of debate and active research [4]. Several mechanisms have been put forward as the probable cause of the droop, such as defects [5, 6], carrier delocalization and recombination at dislocations [7], carrier leakage out of the active region [8, 9], poor hole injection [10], Auger recombination [11–16] or a combination of them [17, 18]. Auger recombination, in particular, is challenging to address because it is an intrinsic nonradiative recombination process of the material (figure 1(b)). The work of Shen *et al* [12] identified Auger recombination as the likely cause of the droop after they observed nonthermal efficiency rollover in optically pumped quasibulk nitride samples. This work stimulated a number of subsequent studies and its findings were subsequently verified in a range of nitride LEDs and lasers by several other groups [14–16, 19–22]. More recently, Iveland *et al* [23] used electron emission spectroscopy to directly observe the generation of Auger electrons in a nitride LED under electrical injection conditions. They also observed a linear correlation between the Auger electron current and the missing current due to efficiency droop, thus providing further evidence for the Auger hypothesis as the leading cause of the efficiency reduction. Further insights are needed in order to better understand the microscopic mechanisms involved in Auger recombination in the nitrides and to devise engineering strategies to mitigate its impact, which can be obtained either by experimental studies or by theoretical simulations.

Despite the abundant experimental evidence, Auger recombination remains an issue of disagreement because of discrepancies between experimental and theoretical data. Early

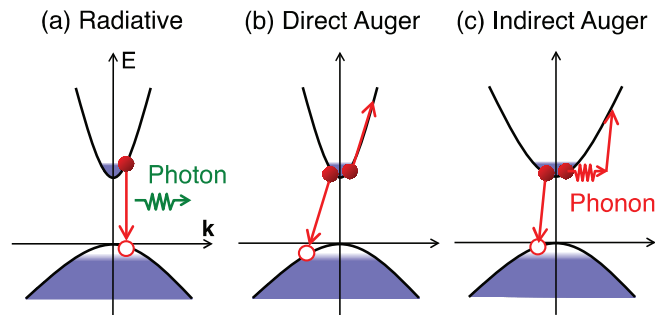


**Figure 1.** Schematic diagram of carrier recombination processes in semiconductors. (a) Radiative recombination occurs vertically in the band-structure diagram and enables photon emission in light-emitting diodes. (b) Auger recombination, a three-particle nonradiative recombination mechanism becomes important at high carrier concentrations and reduces the efficiency of the device. (c) In wide-band-gap semiconductors such as the group-III-nitrides the dominant Auger processes are indirect, assisted by a carrier-scattering mechanism such as electron–phonon coupling or alloy scattering.

calculations by Hader *et al* [24] found that direct Auger recombination is too weak in nitride LEDs to account for the observed droop, a finding that was subsequently verified by other theoretical work [25]. However, Bulashevich and Karpov [26] used the general trend of Auger coefficients for various semiconductors to argue that Auger recombination in the nitrides must occur via higher-order indirect processes such as those assisted by the coupling of electrons to lattice vibrations (figure 1(c)). The significance of phonon-assisted Auger recombination was also predicted by Laubsch *et al* [15]. Preliminary calculations by Pasenow *et al* [27] found that phonon-assisted Auger is stronger than the direct process in the nitrides but they did not report values for the phonon-assisted coefficients. Hader *et al* [5] mentioned preliminary results which indicate that phonon-assisted Auger is not strong enough to explain experiment but they did not report further details. However, these early calculations were based on simple models for the band structure and the electron–phonon interaction, which did not account for all possible indirect Auger transitions.

Our own previous calculations of indirect Auger recombination in the nitrides [28] employed first-principles computational methods based on density functional theory (DFT), a predictive method that can account for all electron states and phonon modes involved in indirect Auger transitions. We found that indirect Auger recombination is indeed strong in the nitrides and that the values of the calculated indirect Auger coefficients were in good agreement with experiment. Thus, our calculations support the hypothesis that Auger recombination is the likely cause of the droop.

In this work, we present insights gained from first-principles calculations on the effects of quantum confinement, temperature and increasing carrier density on the radiative and Auger recombination coefficients and the internal quantum efficiency (IQE) of nitride LEDs. The results on temperature and carrier-density dependence are presented here for the first time. In section 2 we discuss indirect Auger recombination, assisted by electron–phonon coupling and alloy scattering, in bulk nitride materials. In section 3 we describe the effect of the polarization fields that appear in polar devices on the recombination rates and their effect on the

efficiency droop. In section 4 we describe our first-principles formalism for the calculation of the radiative recombination rates in nitrides. Last, in section 5 we discuss the effect of temperature, polarization fields and phase-space filling (PSF) on the recombination rates and the efficiency of an  $\text{In}_{0.15}\text{Ga}_{0.85}\text{N}$  single-quantum-well device.

## 2. Auger recombination in nitride semiconductors

The recombination rate of carriers in a single-quantum-well device is given by the so-called *ABC* model

$$\frac{dn}{dt} = \frac{J}{ed} - An - Bn^2 - Cn^3, \quad (1)$$

where  $J/ed$  is the carrier injection rate,  $J$  is the injected current density,  $d$  is the quantum-well width,  $An$  is the Shockley–Read–Hall recombination rate,  $Bn^2$  is the rate of radiative recombination and  $Cn^3$  is the Auger recombination rate. At steady state, the relation between the current and carrier densities is given by

$$J = ed(An + Bn^2 + Cn^3). \quad (2)$$

At high current densities (high carrier densities) the Auger mechanism becomes the dominant recombination process, which leads to nonradiative carrier loss and reduced high-power efficiency. The IQE of the device  $\eta$  is given by the ratio of the carriers that recombine radiatively over the total recombination rate

$$\eta = \frac{Bn^2}{An + Bn^2 + Cn^3}. \quad (3)$$

At high carrier concentrations the Auger term dominates in the denominator and leads to a reduction of the IQE for high carrier concentrations.

The Auger recombination rate is determined by Fermi's golden rule

$$R_{\text{Auger}} = 2 \frac{2\pi}{\hbar} \sum_{1234} P_{1234} |M_{1234}|^2 \delta(\varepsilon_1 + \varepsilon_2 - \varepsilon_3 - \varepsilon_4), \quad (4)$$

where  $\mathbf{1} \equiv (n_1, \mathbf{k}_1)$ , etc are composite band and wave-vector indices,  $P_{1234} = f_1 f_2 (1 - f_3)(1 - f_4)$  is a statistics factor that accounts for fermionic occupation numbers, and the delta function ensures the overall energy conservation. The electron–electron scattering matrix elements are given in terms of the screened Coulomb interaction  $W(\mathbf{r}, \mathbf{r}')$ ,

$$|M_{1234}|^2 = |\langle \mathbf{12} | W | \mathbf{34} \rangle - \langle \mathbf{12} | W | \mathbf{43} \rangle|^2 + |\langle \mathbf{12} | W | \mathbf{34} \rangle|^2 + |\langle \mathbf{12} | W | \mathbf{43} \rangle|^2,$$

where

$$\langle \mathbf{12} | W | \mathbf{34} \rangle = \iint \psi_1^*(\mathbf{r}) \psi_2^*(\mathbf{r}') \psi_3(\mathbf{r}) \psi_4(\mathbf{r}') W(\mathbf{r}, \mathbf{r}') d\mathbf{r} d\mathbf{r}'$$

and both direct and exchange terms due to fermionic exchange are taken into account.

The corresponding equations for phonon-assisted Auger recombination are similar to the direct case, with appropriate modifications for the matrix elements, energy and momentum conservation and statistics factors. The indirect Auger recombination rate is given by

$$R_{\text{Auger}}^{\text{indirect}} = 2 \frac{2\pi}{\hbar} \sum_{1234, \nu \mathbf{q}} \tilde{P}_{1234, \nu \mathbf{q}} |\tilde{M}_{1234, \nu \mathbf{q}}|^2 \delta(\varepsilon_1 + \varepsilon_2 - \varepsilon_3 - \varepsilon_4 \mp \hbar \omega_{\nu \mathbf{q}}),$$

where  $\tilde{P}_{1234} = f_1 f_2 (1 - f_3)(1 - f_4) (n_{\nu\mathbf{q}} + \frac{1}{2} \pm \frac{1}{2})$  are the modified statistics factors,  $n_{\nu\mathbf{q}}$  are the Bose–Einstein phonon occupation numbers,  $\hbar\omega_{\nu\mathbf{q}}$  are the vibrational frequencies of phonon mode  $\nu$  with wave vector  $\mathbf{q}$ ,  $\tilde{M}$  are the modified matrix elements and the upper (lower) sign corresponds to the process assisted by phonon emission (absorption). The modified Auger matrix elements are given in terms of the direct Auger matrix and the electron–phonon coupling matrix elements. For example, one of the terms contributing to the total matrix element is

$$\tilde{M}_{1234,\nu\mathbf{q}} = \sum_{\mathbf{m}} \frac{\langle \mathbf{12} | W | \mathbf{3m} \rangle g_{\mathbf{m4},\nu\mathbf{q}}}{\varepsilon_{\mathbf{m}} - \varepsilon_{\mathbf{4}} \pm \hbar\omega_{\nu\mathbf{q}}}, \quad (5)$$

where  $g_{\mathbf{m4},\nu\mathbf{q}} = \langle \mathbf{m} | \partial_{\nu\mathbf{q}} V | \mathbf{4} \rangle$  are the electron–phonon coupling matrix elements from state  $\mathbf{m}$  to state  $\mathbf{4}$  due to the perturbation of the crystal potential  $V$  by the phonon mode ( $\nu\mathbf{q}$ ). There are a total of eight terms similar to (5), which account for all possible combinations of the electron–phonon coupling and Auger Feynman diagrams that need to be considered. All terms are calculated with consistent wave-function phases in order to properly account for quantum-interference effects among the various quantum processes.

First-principles calculations for the indirect Auger coefficients in GaN and InGaN were performed with DFT and related techniques [29]. The carrier energies and wave functions are calculated with DFT and the local-density approximation for the exchange-correlation potential [30, 31]. The band gap is adjusted with a rigid scissors shift to correct for the band-gap underestimation problem of DFT. The static dielectric function involved in the screened-Coulomb-interaction matrix elements is evaluated using the model of Cappellini *et al* [32]. The phonon frequencies and electron–phonon coupling matrix elements are calculated using density functional perturbation theory [33]. Calculations for the phonon-assisted coefficient are performed for bulk GaN and extrapolated to other alloy compositions by adjusting the band-gap value through the scissors shift. As pointed out in [34], the denominator in (5) may become equal to zero for resonant direct transitions to intermediate states. An imaginary component with a value equal to 0.3 eV was added to the intermediate-state energies in the denominator of (5) in order to numerically handle singularities due to such resonant direct transitions. The value of this broadening parameter does not affect the calculated phonon-assisted Auger recombination rates in the nitrides. This is because the intermediate states involved in the calculation of (5) are far from resonance for all band-gap values and the real part of the energy denominator dominates. Therefore, the theoretical treatment of phonon-assisted Auger recombination in terms of second-order perturbation theory yields results that do not significantly depend on the chosen value of this imaginary broadening parameter. The alloy-scattering-assisted Auger coefficients are calculated for the special quasirandom structure (SQS) [35] of  $\text{In}_{0.25}\text{Ga}_{0.75}\text{N}$  and are extrapolated to other alloy compositions using the dependence of the alloy-scattering potential on the composition,  $C(x) \propto x(1 - x)$ .

Our calculated results for the phonon- and alloy-scattering-assisted Auger coefficients have been reported elsewhere [28]. Here we briefly review the results and compare with subsequent work. The cumulative value of the indirect Auger coefficients is in the range of  $1.5\text{--}3.0 \times 10^{-31} \text{ cm}^6 \text{ s}^{-1}$  for alloys with In composition in the 10–25% range, which is in good agreement with experimental measurements. The dominant carrier scattering mechanisms are short-range electron–phonon coupling and alloy scattering, while scattering by charged defects is not important for realistic defect densities. These findings are consistent with our own earlier work on free-carrier absorption in the nitrides [36, 37] which found that electron–phonon

coupling and alloy scattering are particularly strong in nitride semiconductors. Our results have since been validated by experimental measurements (e.g. [21, 38]).

Subsequent theoretical work by Bertazzi *et al* [34] found values much lower than our calculated results and argued that phonon-assisted Auger recombination in the nitrides may only be relevant in low-band-gap alloys (yellow-green). However, these calculations include the electron–phonon interaction only as a lifetime-broadening mechanism that relaxes the energy conservation requirement in (4). However, a complete theory of phonon-assisted Auger recombination needs to take into account the modification of the Auger transition probabilities due to interaction of the charge carriers with the lattice. Since the work of Bertazzi *et al* [34] did not consider the modification of the Auger matrix elements due to the electron–phonon interaction, it is not expected to yield accurate phonon-assisted Auger coefficients.

The dependence of the Auger coefficient on the carrier density plays a role in the LED efficiency. The Auger coefficient  $C$  is obtained by dividing the recombination rate per unit volume by the third power of the carrier density,  $C = R_{\text{Auger}}/n^3 V$ . For low carrier concentrations the recombination rate is proportional to the cube of the concentration of free carriers and the  $C$  coefficient is independent of carrier density. However, the semiconductor becomes degenerate at high carrier concentrations and the  $C$  coefficient becomes a monotonically decreasing function of the carrier density. This effect is known as phase-space filling [39] and, like the effect of polarization fields [40], decreases LED efficiency because it increases the operating carrier density for a given current density. The effect of PSF on quantum efficiency is discussed in further detail in section 5.

The Auger coefficients are also a function of the temperature of the material. The temperature dependence reported in our previous work [28] arises both from the phonon occupation numbers and the carrier distribution over the electronic states around the conduction-band minimum. Both phonon- and alloy-scattering-assisted Auger coefficients depend on temperature. Moreover, phonon-emission processes enable phonon-assisted Auger recombination even at absolute zero temperature, which explains reported experimental results for droop at very low temperatures [41]. Other effects such as lattice expansion or the temperature dependence of the band structure may play a secondary role but were not explicitly considered in our work.

### 3. Auger recombination in quantum wells

Although the discussion of indirect Auger recombination in the previous section applies to bulk materials, the recombination rates of carriers in quantum wells in the active region of LEDs are affected by quantum confinement. The polarization fields that develop in quantum wells keep the electron and hole wave functions apart and reduce the recombination rates. Moreover, the lack of momentum conservation along the confinement direction constitutes an additional scattering mechanism that enables Auger transitions [42]. Quantum confinement affects the electron and phonon energies as well as the electron–phonon and electron–electron scattering matrix elements. The full analysis of carrier recombination rates in nitride quantum wells requires calculations that can predict the modification of electron and phonon properties by quantum confinement at the microscopic level using first-principles theory. Recently,  $k \cdot p$  calculations have shown that Auger recombination in narrow nitride quantum wells increases by quantum confinement [43]. In the following analysis, we assume that quantum confinement does not significantly modify the bulk recombination rates and that the main effect

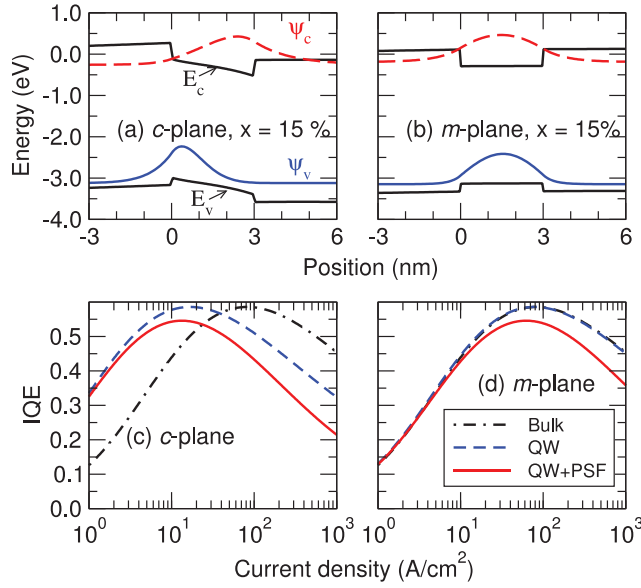


**Figure 2.** Valence ( $E_v$ ) and conduction ( $E_c$ ) band profiles and electron ( $\psi_c$ ) and hole ( $\psi_v$ ) wave functions of a (a)  $c$ -plane and a (b)  $m$ -plane light-emitting diode consisting of a single 3 nm-wide  $\text{In}_{0.15}\text{Ga}_{0.85}\text{N}$  quantum well. The electron–hole wave-function overlap is larger in the  $m$ -plane quantum well and improves the high-power efficiency of the  $m$ -plane device (d) compared to the  $c$ -plane case (c). PSF reduces the values of the recombination coefficients at high carrier concentrations and exacerbates the efficiency droop.

of the confinement is the spatial separation of the electron and hole wave functions by the polarization fields.

The polarization fields in the active region of polar nitride quantum wells reduce the carrier recombination rates. It has been shown that the radiative rate of carriers in the quantum well  $B_{\text{QW}}$  is proportional to the electron–hole wave-function overlap squared,  $B_{\text{QW}} = B_{\text{Bulk}}|F_{\text{cv}}|^2$ , where  $B_{\text{Bulk}}$  is the coefficient in the bulk and

$$F_{\text{cv}} = \int \psi_c(z)\psi_v(z)dz$$

is the overlap between the electron and hole envelope functions, assuming that quantum confinement is along the  $z$  direction [44]. In previous work, we derived that the Shockley–Read–Hall and Auger coefficients are also proportional to the electron–hole overlap squared,  $A_{\text{QW}} = A_{\text{Bulk}}|F_{\text{cv}}|^2$  and  $C_{\text{QW}} = C_{\text{Bulk}}|F_{\text{cv}}|^2$  [40]. Thus, the recombination rates decrease by the same ratio as the wave-function overlap decreases due to polarization fields and the IQE as a function of *carrier* density is unaffected by quantum confinement. However, when the efficiency is plotted as a function of the *current* density using (2) it displays significantly stronger droop when the electron–hole overlap is weak (figures 2(a) and (c)). This is because the reduction of the recombination rates by the polarization fields increases the steady-state carrier density in the device for a given current density and increases the fraction of carriers that recombine via the Auger mechanism.

The fact that the polarization fields increase the fraction of carriers lost to Auger recombination and aggravate the droop behavior has also been reported experimentally. David

and Grundmann [45] demonstrated that increasing polarization fields in polar LEDs of higher In content aggravate the IQE versus *current* density curves, even though the IQE versus *carrier* density curves show similar droop. Zhao *et al* [46] reported that InGaN QWs with high electron–hole overlap exhibit improved efficiency. Pan *et al* [47] used a semipolar growth direction to fabricate a high-power low-droop blue LED. Reducing or eliminating the polarization fields and the associated electron–hole spatial separation is therefore a viable strategy for mitigating the droop.

#### 4. Radiative recombination

Spontaneous radiative recombination is the fundamental microscopic quantum process that leads to light emission in semiconductors and the operation of LEDs (figure 1(a)). The rate of spontaneous recombination  $R_{\text{sp}}$  is calculated using Fermi’s golden rule and the electron–photon coupling Hamiltonian matrix elements [48]

$$R_{\text{sp}}(n, T) = \frac{8n_r e^2}{c^3 \hbar^2} \sum_{\text{cvk}} f_{\text{ck}}(1 - f_{\text{vk}})(\varepsilon_{\text{ck}} - \varepsilon_{\text{vk}}) \frac{|\vec{v}_{\text{cvk}}|^2}{3}, \quad (6)$$

where  $n_r$  is the refractive index and  $|\vec{v}_{\text{cvk}}|^2/3$  is the directionally averaged squared velocity-operator matrix element for an optical transition between the valence and conduction band at wave vector  $\mathbf{k}$ . This is the general equation for Fermi–Dirac statistics. In the limiting case of carriers in nondegenerate semiconductors (6) reduces to the result given by Boltzmann statistics [49]. The radiative coefficient  $B$  is obtained by dividing the recombination rate per unit volume with the carrier density squared,  $B = R_{\text{sp}}/n^2 V$ .

The radiative recombination rate in (6) is determined from first-principles calculations based on DFT [29]. The electronic energy eigenvalues are calculated with the local-density approximation [30, 31] and the band gap is adjusted to the experimental value using a rigid scissors shift. The calculation of the radiative rate in (6) requires the band energies and velocities on a very fine mesh of points near the conduction- and valence-band extrema. These can be determined very efficiently using the maximally localized Wannier function (MLWF) method [50, 51]. First, the band energies are determined on a uniform mesh of points in the first Brillouin zone ( $8 \times 8 \times 8$  in the case of GaN and  $4 \times 4 \times 4$  for the case of the  $\text{In}_{0.25}\text{Ga}_{0.75}\text{N}$  special quasirandom structure [35]). Subsequently, the band energies are interpolated with the MLWF method to fine meshes of points in the Brillouin zone (as fine as  $70 \times 70 \times 35$  for GaN and  $50 \times 50 \times 20$  for the  $\text{In}_{0.25}\text{Ga}_{0.75}\text{N}$  SQS cell are needed to achieve convergence) in order to determine the carrier quasi-Fermi levels as a function of free-carrier density and temperature. The interband velocity matrix elements are also calculated on these fine meshes of points using the MLWF method [52] and adjusted for the band-gap correction in order to preserve the sum rule for the imaginary part of the dielectric function [53]. We have recently applied a similar approach to calculate the phonon-assisted optical absorption spectrum of silicon [54]. The refractive-index values for GaN and the  $\text{In}_{0.25}\text{Ga}_{0.75}\text{N}$  SQS structure were determined using the model of Bergmann *et al* [55].

Our calculated values for the radiative coefficient of GaN and  $\text{In}_{0.25}\text{Ga}_{0.75}\text{N}$  are plotted as a function of carrier concentration and temperature in figures 3(a) and (b). At high carrier concentrations where Fermi–Dirac carrier statistics apply, the coefficients decrease due to

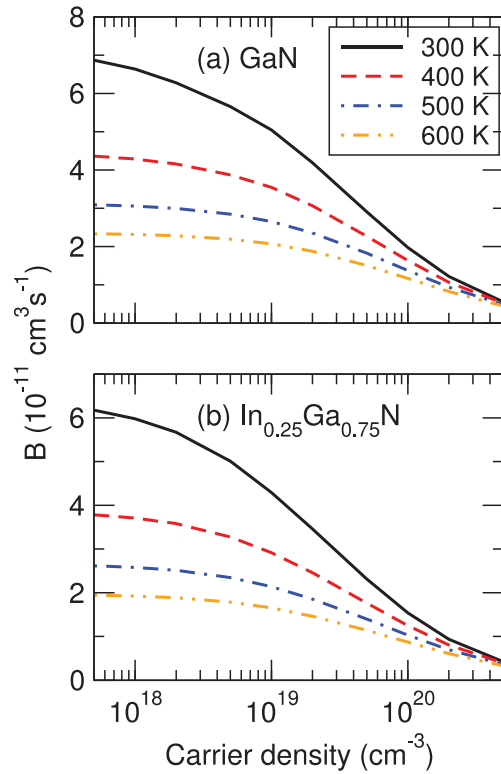


**Figure 3.** Radiative recombination  $B$  of (a) GaN and (b)  $\text{In}_{0.25}\text{Ga}_{0.75}\text{N}$  plotted as a function of carrier concentration and temperature. The coefficients decrease at high carrier concentrations due to PSF effects.

PSF [39]. In the plotted carrier-concentration range the coefficients can be fitted by a function of the form

$$B(n) = \frac{B_0}{1 + (n/n_0)^b}, \quad (7)$$

where  $B_0$  is the low-density limit of the coefficient,  $n_0$  is the characteristic carrier density for the onset of PSF and  $b$  is a dimensionless exponent. At 300 K the fitted coefficients are  $B_0 = 7.1 \times 10^{-11} \text{ cm}^3 \text{ s}^{-1}$ ,  $n_0 = 3.0 \times 10^{19} \text{ cm}^{-3}$  and  $b = 0.80$  for GaN, while for  $\text{In}_{0.25}\text{Ga}_{0.75}\text{N}$  these values are  $B_0 = 6.4 \times 10^{-11} \text{ cm}^3 \text{ s}^{-1}$ ,  $n_0 = 2.4 \times 10^{19} \text{ cm}^{-3}$  and  $b = 0.82$ . These numbers are in agreement with experimentally determined values [14]. We observe that the  $B$  coefficient of  $\text{In}_{0.25}\text{Ga}_{0.75}\text{N}$  is reduced by 28% when the carrier density increases from  $10^{18}$  to  $10^{19} \text{ cm}^{-3}$ , within the range of operation of LEDs. For all carrier concentrations the coefficients are decreasing as a function of temperature.

## 5. Discussion

The magnitude of the indirect Auger coefficients as determined from our first-principles calculations for bulk nitrides is in good agreement with experimental measurements. The cumulative values we obtained are in the range of  $1.5\text{--}3.0 \times 10^{-31} \text{ cm}^6 \text{ s}^{-1}$  for alloys with In composition in the 10–25% range, which is in good agreement with reported experimental

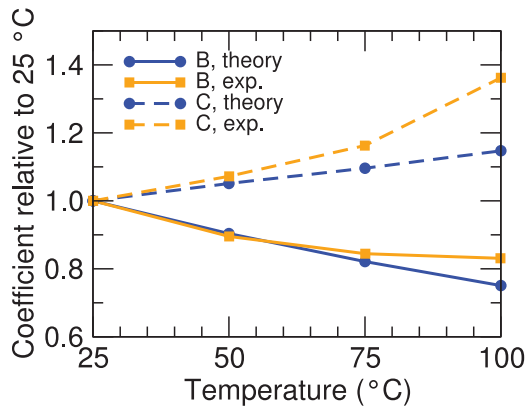


**Figure 4.** Relative temperature dependence of the radiative  $B$  and the Auger  $C$  coefficients of  $\text{In}_{0.15}\text{Ga}_{0.85}\text{N}$  as calculated from first-principles theory and measured experimentally. The experimental data are from [38].

results [12, 14, 21, 38]. This agreement indicates that indirect Auger recombination assisted by electron–phonon coupling and alloy scattering is important in nitride LEDs and is the likely cause of the droop.

We examined the temperature dependence of the Auger and radiative coefficients. Figure 4 illustrates the relative temperature dependence of the radiative and indirect Auger coefficients of bulk  $\text{In}_{0.15}\text{Ga}_{0.85}\text{N}$  compared to the values at 25 °C as calculated by our theory and measured in experiment [38]. The theoretical values are calculated for a carrier concentration of  $10^{19} \text{ cm}^{-3}$ . The temperature dependence of both phonon- and alloy-scattering-assisted Auger processes is considered. The theoretical values of the alloy-assisted coefficient are linearly interpolated from the data for  $\text{In}_{0.25}\text{Ga}_{0.75}\text{N}$  at 300 and 600 K while using the dependence of the alloy-scattering potential on the alloy composition  $C(x) \propto x(1-x)$ . The theoretical data for the phonon-assisted coefficients are obtained from the GaN data by adjusting the band gap with a scissors shift to the value corresponding to the 15% In composition (2.9 eV [56]). The temperature dependence in the phonon-assisted case arises from the increased thermal occupation of the vibrational modes at higher temperatures. Effects on the band structure due to thermal expansion or electron–phonon coupling were not considered in this study.

The temperature dependence of our calculated Auger coefficients is in good agreement with experiment, which further validates the role of indirect Auger processes. A full analysis of the temperature dependence of the efficiency droop requires the comparison of the temperature dependence of the entire IQE curve between theory and experiment. However, it is difficult to compare theoretical and experimental features of the IQE curve, such as the position and magnitude of the peak efficiency, because they depend directly on the value of the Shockley–Read–Hall coefficient, which is sample-dependent. Hence, general conclusions of the temperature-dependence of droop can be drawn only from the effect of temperature on the radiative and Auger coefficients. Figure 4 illustrates that the radiative coefficient decreases while the Auger coefficient increases for increasing temperature, which both have a negative effect on the droop. The direct Auger recombination coefficient depends exponentially on temperature, while indirect Auger coefficients exhibit weak temperature dependence [57]. This is because increasing temperature enables momentum-conserving direct transitions to a wider range of final states. In the indirect case, however, additional momentum is provided by the phonons or

the alloy-scattering potential. Thus, a higher temperature is not needed to enable momentum conservation for indirect Auger transitions. Our calculated results for indirect Auger in figure 4 display a weak temperature dependence, in agreement with the experimentally observed nonexponential temperature dependence. Moreover, the work of Laubsch *et al* [41] found a weak temperature dependence of the IQE curve at high current densities and measured identical values for the Auger coefficient at 300 and at 4 K, [15] which suggests that the weak temperature dependence also extends to low temperatures. These observations support the argument that the dominant Auger processes are indirect. Moreover, the radiative coefficient decreases with temperature in a way similar to the theoretical dependence predicted for nondegenerate carriers,  $B(T) \sim T^{-3/2}$ .

Although the theoretical and experimental curves in figure 4 somewhat deviate at high temperatures, the ratio of the radiative to the Auger rate is similar. For example, the experimental relative  $B/B(25^\circ\text{C})-C/C(25^\circ\text{C})$  ratio at  $100^\circ\text{C}$  is 0.61 while the theoretical one is 0.65, thus the difference is only 7%. We attribute the remaining differences between the data to the uncertainties in the experimental determination of the  $B$  and  $C$  coefficients and the omission of temperature-dependent effects in the theoretical calculations, such as thermal expansion and the temperature dependence of the band gap.

Polarization fields negatively impact LED efficiency. Figures 2(c) and (d) illustrate the IQE for a polar and a nonpolar LED device consisting of a single 3 nm-wide  $\text{In}_{0.15}\text{Ga}_{0.85}\text{N}$  quantum well. The recombination rates as a function of electron-hole wave-function overlap were calculated as in section 3. The values of the bulk recombination coefficients were taken from experimental measurements as in [40]. The efficiency droop is stronger in the polar-LED case because the reduction of the recombination rates by the electron-hole separation (figures 2(a) and (b)) increases the steady-state carrier density in the quantum well and thus the fraction of carriers that recombine by the Auger process.

Phase-space-filling effects are also important for the efficiency droop. Figures 2(c) and (d) illustrate the effect of PSF on the efficiency curves of a polar and a nonpolar LED. To describe PSF in the calculation of the IQE versus current curves, we used the model of (7) to describe the reduction of the  $B$  and  $C$  coefficients at higher carrier densities. The model parameters in the evaluation of (7) were taken from experimental measurements ( $n_0 = 2.0 \times 10^{19} \text{ cm}^{-3}$  and  $b = 1.0$  [14]), which agree with our calculated values for the phase-space-filling behavior of the radiative coefficient. Just like polarization fields, PSF reduces the recombination rates and increases the carrier density in the quantum well for a given current density. As a result, a larger fraction of carriers recombine via Auger for a fixed current density when PSF is taken into account, and that is reflected in the reduction of the efficiency both in polar and in nonpolar devices. The data in figures 2(c) and (d) do not include the effect of screening of the polarization fields by the free carriers, but our conclusions on the effect of PSF on the IQE must remain true even when these fields are taken into account.

## 6. Conclusion

In conclusion, we used first-principles computational methods to analyze the dependence of the radiative and Auger coefficients in nitrides as a function of temperature, carrier density and polarization fields. The temperature dependence of the calculated coefficients is in good agreement with experiment, which further demonstrates that Auger recombination is important in LEDs and the likely cause of the droop. Polarization fields and PSF negatively impact

device efficiency and need to be addressed for the engineering of high-efficiency high-power nitride LEDs.

## Acknowledgments

We thank Patrick Rinke, Kris Delaney, Audrius Alkauskas, James Speck, Claude Weisbuch and Aurélien David for useful discussions. EK and DS were supported as part of the Center for Energy Efficient Materials, an Energy Frontier Research Center funded by the US Department of Energy, Office of Basic Energy Sciences under Award no. DE-SC0001009. QY was supported by the UCSB Solid State Lighting and Energy Center. Computational resources were provided by the Center for Scientific Computing at the CNSI and MRL (an NSF MRSEC, DMR-1121053) (NSF CNS-0960316) and the National Energy Research Scientific Computing Center, which is supported by the Office of Science of the US Department of Energy under contract no. DE-AC02-05CH11231.

## References

- [1] Pimputkar S, Speck J S, DenBaars S P and Nakamura S 2009 Prospects for LED lighting *Nature Photon.* **3** 180–2
- [2] Nakamura S, Senoh M and Mukai T 1993 High-power InGaN/GaN double-heterostructure violet light emitting diodes *Appl. Phys. Lett.* **62** 2390–2
- [3] Humphreys C J 2008 Solid state lighting *MRS Bull.* **33** 459–70
- [4] Piprek J 2010 Efficiency droop in nitride-based light-emitting diodes *Phys. Status Solidi a* **207** 2217–25
- [5] Hader J, Moloney J V and Koch S W 2010 Density-activated defect recombination as a possible explanation for the efficiency droop in GaN-based diodes *Appl. Phys. Lett.* **96** 221106
- [6] Bochkareva N I, Voronenkov V V, Gorbunov R I, Zubrilov A S, Lelikov Y S, Latyshev F E, Rebane Y T, Tsyuk A I and Shreter Y G 2010 Mechanism of the GaN LED efficiency falloff with increasing current *Semiconductors* **44** 794–800
- [7] Monemar B and Sernelius B E 2007 Defect related issues in the ‘current roll-off’ in InGaN based light emitting diodes *Appl. Phys. Lett.* **91** 181103
- [8] Kim M-H, Schubert M F, Dai Q, Kim J K, Schubert E F, Piprek J and Park Y 2007 Origin of efficiency droop in GaN-based light-emitting diodes *Appl. Phys. Lett.* **91** 183507
- [9] Dai Q, Shan Q, Wang J, Chhajed S, Cho J, Schubert E F, Crawford M H, Koleske D D, Kim M-H and Park Y 2010 Carrier recombination mechanisms and efficiency droop in GaInN/GaN light-emitting diodes *Appl. Phys. Lett.* **97** 133507
- [10] Xie J, Ni X, Fan Q, Shimada R, Özgür U and Morkoç H 2008 On the efficiency droop in InGaN multiple quantum well blue light emitting diodes and its reduction with p-doped quantum well barriers *Appl. Phys. Lett.* **93** 121107
- [11] Gardner N F, Müller G O, Shen Y C, Chen G, Watanabe S, Götz W and Krames M R 2007 Blue-emitting InGaN–GaN double-heterostructure light-emitting diodes reaching maximum quantum efficiency above  $200 \text{ A cm}^{-2}$  *Appl. Phys. Lett.* **91** 243506
- [12] Shen Y C, Mueller G O, Watanabe S, Gardner N F, Munkholm A and Krames M R 2007 Auger recombination in InGaN measured by photoluminescence *Appl. Phys. Lett.* **91** 141101
- [13] Maier M, Köhler K, Kunzer M, Pletschen W and Wagner J 2009 Reduced nonthermal rollover of wide-well GaInN light-emitting diodes *Appl. Phys. Lett.* **94** 041103
- [14] David A and Grundmann M J 2010 Droop in InGaN light-emitting diodes: a differential carrier lifetime analysis *Appl. Phys. Lett.* **96** 103504

- [15] Laubsch A, Sabathil M, Baur J, Peter M and Hahn B 2010 High-power and high-efficiency InGaN-based light emitters *IEEE Trans. Electron Devices* **57** 79–87
- [16] Phillips W A, Thrush E J, Zhang Y and Humphreys C J 2012 Studies of efficiency droop in GaN based LEDs *Phys. Status Solidi c* **9** 765–9
- [17] Saguatti D, Bidinelli L, Verzellesi G, Member S, Meneghini M, Meneghesso G, Zanoni E, Butendeich R and Hahn B 2012 Investigation of efficiency-droop mechanisms in multi-quantum-well InGaN/GaN blue light-emitting diodes *IEEE Trans. Electron Devices* **59** 1402–9
- [18] Deppner M, Römer F and Witzigmann B 2012 Auger carrier leakage in III-nitride quantum-well light emitting diodes *Phys. Status Solidi Rapid Res. Lett.* **6** 418–20
- [19] Zhang M, Bhattacharya P, Singh J and Hinckley J 2009 Direct measurement of auger recombination in  $\text{In}_{0.1}\text{Ga}_{0.9}\text{N}/\text{GaN}$  quantum wells and its impact on the efficiency of  $\text{In}_{0.1}\text{Ga}_{0.9}\text{N}/\text{GaN}$  multiple quantum well light emitting diodes *Appl. Phys. Lett.* **95** 201108
- [20] Meneghini M, Trivellini N, Meneghesso G, Zanoni E, Zehnder U and Hahn B 2009 A combined electro-optical method for the determination of the recombination parameters in InGaN-based light-emitting diodes *J. Appl. Phys.* **106** 114508
- [21] Scheibenzuber W G, Schwarz U T, Sulmoni L, Dorsaz J, Carlin J-F and Grandjean N 2011 Recombination coefficients of GaN-based laser diodes *J. Appl. Phys.* **109** 093106
- [22] Brendel M, Kruse A, Jönen H, Hoffmann L, Bremers H, Rossow U and Hangleiter A 2011 Auger recombination in GaInN/GaN quantum well laser structures *Appl. Phys. Lett.* **99** 031106
- [23] Iveland J, Martinelli L, Peretti J, Speck J S and Weisbuch C 2013 Direct measurement of Auger electrons emitted from a semiconductor light-emitting diode under electrical injection: identification of the dominant mechanism for efficiency droop *Phys. Rev. Lett.* **110** 177406
- [24] Hader J, Moloney J V, Pasenow B, Koch S W, Sabathil M, Linder N and Lutgen S 2008 On the importance of radiative and Auger losses in GaN-based quantum wells *Appl. Phys. Lett.* **92** 261103
- [25] Bertazzi F, Goano M and Bellotti E 2010 A numerical study of Auger recombination in bulk InGaN *Appl. Phys. Lett.* **97** 231118
- [26] Bulashevich K A and Karpov S Y 2008 Is Auger recombination responsible for the efficiency rollover in III-nitride light-emitting diodes? *Phys. Status Solidi c* **5** 2066–9
- [27] Pasenow B, Koch S W, Hader J, Moloney J V, Sabathil M, Linder N and Lutgen S 2009 Auger losses in GaN-based quantum wells: microscopic theory *Phys. Status Solidi c* **6** S864–8
- [28] Kioupakis E, Rinke P, Delaney K T and Van de Walle C G 2011 Indirect Auger recombination as a cause of efficiency droop in nitride light-emitting diodes *Appl. Phys. Lett.* **98** 161107
- [29] Martin R M 2004 *Electronic Structure: Basic Theory and Practical Methods* (Cambridge: Cambridge University Press)
- [30] Ceperley D M and Alder B J 1980 Ground state of the electron gas by a stochastic method *Phys. Rev. Lett.* **45** 566–9
- [31] Perdew J and Zunger A 1981 Self-interaction correction to density-functional approximations for many-electron systems *Phys. Rev. B* **23** 5048
- [32] Cappellini G, Del Sole R, Reining L and Bechstedt F 1993 Model dielectric function for semiconductors *Phys. Rev. B* **47** 9892–5
- [33] Baroni S, de Gironcoli S, Dal Corso A and Giannozzi P 2001 Phonons and related crystal properties from density-functional perturbation theory *Rev. Mod. Phys.* **73** 515
- [34] Bertazzi F, Goano M and Bellotti E 2012 Numerical analysis of indirect Auger transitions in InGaN *Appl. Phys. Lett.* **101** 011111
- [35] Shin D, Arróyave R, Liu Z-K and Van de Walle A 2006 Thermodynamic properties of binary hcp solution phases from special quasirandom structures *Phys. Rev. B* **74** 024204
- [36] Kioupakis E, Rinke P, Schleife A, Bechstedt F and Van de Walle C G 2010 Free-carrier absorption in nitrides from first principles *Phys. Rev. B* **81** 241201
- [37] Kioupakis E, Rinke P and Van de Walle C G 2010 Determination of internal loss in nitride lasers from first principles *Appl. Phys. Express* **3** 082101

- [38] Galler B, Drechsel P, Monnard R, Rode P, Stauss P and Froehlich S 2012 Influence of indium content and temperature on Auger-like recombination in InGaN quantum wells grown on (111) silicon substrates *Appl. Phys. Lett.* **101** 131111
- [39] Hader J, Moloney J V and Koch S W 2005 Suppression of carrier recombination in semiconductor lasers by phase-space filling *Appl. Phys. Lett.* **87** 201112
- [40] Kioupakis E, Yan Q and Van de Walle C G 2012 Interplay of polarization fields and Auger recombination in the efficiency droop of nitride light-emitting diodes *Appl. Phys. Lett.* **101** 231107
- [41] Laubsch A *et al* 2009 On the origin of IQE-‘droop’ in InGaN LEDs *Phys. Status Solidi c* **6** S913–6
- [42] Polkovnikov A and Zegrya G 1998 Auger recombination in semiconductor quantum wells *Phys. Rev. B* **58** 4039–56
- [43] Vaxenburg R, Lifshitz E and Efros A L 2013 Suppression of Auger-stimulated efficiency droop in nitride-based light emitting diodes *Appl. Phys. Lett.* **102** 031120
- [44] Li X, Okur S, Zhang F, Avrutin V, Özgür U, Morkoç H, Hong S M, Yen S H, Hsu T S and Matulionis A 2012 Impact of active layer design on InGaN radiative recombination coefficient and LED performance *J. Appl. Phys.* **111** 063112
- [45] David A and Grundmann M J 2010 Influence of polarization fields on carrier lifetime and recombination rates in InGaN-based light-emitting diodes *Appl. Phys. Lett.* **97** 033501
- [46] Zhao H, Liu G, Zhang J, Poplawsky J D, Dierolf V and Tansu N 2011 Approaches for high internal quantum efficiency green InGaN light-emitting diodes with large overlap quantum wells *Opt. Express* **19** A991–1007
- [47] Pan C-C, Tanaka S, Wu F, Zhao Y, Speck J S, Nakamura S, DenBaars S P and Feezell D 2012 High-power, low-efficiency-droop semipolar (20 $\bar{2}$ 1) single-quantum-well blue light-emitting diodes *Appl. Phys. Express* **5** 062103
- [48] Ridley B 1982 *Quantum Processes in Semiconductors* (Oxford: Clarendon)
- [49] Dmitriev A and Oruzhenikov A 1999 The rate of radiative recombination in the nitride semiconductors and alloys *J. Appl. Phys.* **86** 3241–6
- [50] Marzari N, Mostofi A A, Yates J R, Souza I and Vanderbilt D 2012 Maximally localized Wannier functions: theory and applications *Rev. Mod. Phys.* **84** 1419–75
- [51] Mostofi A A, Yates J R, Lee Y-S, Souza I, Vanderbilt D and Marzari N 2008 Wannier90: a tool for obtaining maximally-localised Wannier functions *Comput. Phys. Commun.* **178** 685–99
- [52] Yates J R, Wang X, Vanderbilt D and Souza I 2007 Spectral and Fermi surface properties from Wannier interpolation *Phys. Rev. B* **75** 195121
- [53] Rohlfling M and Louie S 2000 Electron–hole excitations and optical spectra from first principles *Phys. Rev. B* **62** 4927–44
- [54] Noffsinger J, Kioupakis E, Van de Walle C G, Louie S G and Cohen M L 2012 Phonon-assisted optical absorption in silicon from first principles *Phys. Rev. Lett.* **108** 167402
- [55] Bergmann M J and Casey H C 1998 Optical-field calculations for lossy multiple-layer Al<sub>x</sub>Ga<sub>1-x</sub>N/In<sub>x</sub>Ga<sub>1-x</sub>N laser diodes *J. Appl. Phys.* **84** 1196–203
- [56] Moses P G and Van de Walle C G 2010 Band bowing and band alignment in InGaN alloys *Appl. Phys. Lett.* **96** 021908
- [57] Lochmann W 1977 Phonon-assisted Auger recombination in semiconductors *Phys. Status Solidi a* **40** 285–92